

UV spectroscopic identification and thermodynamic analysis of protonated third strand deoxycytidine residues at neutrality in the triplex $d(C^+-T)_6:[d(A-G)_6 \cdot d(C-T)_6]$; evidence for a proton switch

Laurence Lavelle and Jacques R. Fresco*

Department of Molecular Biology, Princeton University, Princeton, NJ 08544-1014, USA

Received March 28, 1995; Revised and Accepted June 6, 1995

ABSTRACT

Near-UV difference spectral analysis of the triplex formed from $d(C-T)_6$ and $d(A-G)_6 \cdot d(C-T)_6$ in neutral and acidic solution shows that the third strand dC residues are protonated at pH 7.0, far above their intrinsic pK_a . Additional support for ion-dipole interactions between the third strand dC residues and the G·C target base pairs comes from reduced positive dependence of triplet stability on ionic strength below 0.9 M Na⁺, inverse dependence above 0.9 M Na⁺ and strong positive dependence on hydrogen ion concentration. Molecular modeling (AMBER) of C:G·C and C⁺:G·C base triplets with the third strand base bound in the Hoogsteen geometry shows that only the C⁺:G·C triplet is energetically feasible. van't Hoff analysis of the melting of the triplex and target duplex shows that between pH 5.0 and 8.5 in 0.15 M NaCl/0.005 M MgCl₂ the enthalpy of melting (ΔH°_{obs}) varies from 5.7 to 6.6 kcal.mol⁻¹ for the duplex in a duplex mixture and from 7.3 to 9.7 kcal.mol⁻¹ for third strand dissociation in the triplex mixture. We have extended the condensation-screening theory of Manning to pH-dependent third strand binding. In this development we explicitly include the H⁺ contribution to the electrostatic free

energy and obtain $\frac{\partial T_m}{\partial(\ln[H^+])} = \frac{1}{2} \frac{\Delta n_2 R(T_m)^2}{Z_2 \Delta H_2}$. The number of protons released in the dissociation of the third strand from the target duplex at pH 7.0, Δn_2 , is thereby calculated to be 5.5, in good agreement with approximately six third strand dC residues per mole of triplex. This work shows that when third strand binding requires protonated residues that would otherwise be neutral, triplex formation and dissociation are mediated by proton uptake and release, i.e., a proton switch. As a by-product of this study, we have found that at low pH the Watson-Crick duplex $d(A-G)_6 \cdot d(C-T)_6$ undergoes a transition to a parallel Hoogsteen duplex $d(A-G)_6 \cdot d(C^+-T)_6$.

INTRODUCTION

Nucleic acid triplexes hold much current attention, in large measure because of the possibilities for exploiting third strand binding as an artificial mechanism for the control of gene expression (reviewed in 1,2) and as a tool for site specific delivery of reagents to genomes (e.g., 3). It is therefore important to understand the molecular mechanisms that underlie recognition of target base pairs by third strand residues. The targets of interest for third strand binding are Watson-Crick helices with the base pairs A·T/U and G·C, arranged in homopurine·homopyrimidine segments, since it is in such sequences that the target pairs are most strongly and accurately recognized, i.e., bound specifically by third strand residues. In the present work, the issue of primary concern is the way a G·C target pair is recognized by a third strand cytidine residue.

The G·C base pair was originally shown to be bound by third strand C or G residues in studies with polyribonucleotides (4,5). In those studies it was shown that the interaction of C with G·C base pairs is at best weak at neutrality, being considerably stabilized as the pH is decreased. These observations were reinforced in the later studies of Morgan and Wells (6) and Thiele and Guschlbauer (7); the rationale was given clear expression in the model building study of Arnott *et al.* (8), who showed that addition of a proton to N3 of C enables that base to form two rather than one hydrogen bond (H-bond) with G (or I) of a target base pair in the Hoogsteen arrangement, thus forming a base triplet that is isostructural with U:A·U and T:A·T. It is this rationale that has been used to explain the stabilization at low pH of intramolecular triplexes with homopyrimidine third strands i.e., H-DNA (9) and intermolecular triplexes with poly(C) third strands (10).

Since the pK_a of CMP and dCMP are 4.3 and 4.6, respectively, at 25°C, this raises the question of the structure of the C:G·C triplet at neutrality or above, where biologically relevant triplex formation is likely to occur *in vivo*. The question receives added impetus from reports that some dC-rich third strands can bind productively to targets at neutrality or above (11–13). It is also of interest to know whether under physiological conditions C:G·C triplets involve two H-bonds between third strand dC residues

* To whom correspondence should be addressed

and their target dG residues, as has been observed only below pH 6 at very high third strand concentration by NMR (14,15), or instead only one H-bond as the conventional wisdom suggests (e.g., 13,16), i.e., at neutrality the dC residue is neutral. An effort to address this question was made using NMR on a sequence forming a short intramolecular triplex with C:G·C triplets (17). While imino protons on dC residues were observed at neutrality, they could not be quantitated, so that the data was not amenable to thermodynamic analysis. Hence, we undertook a different spectroscopic approach to address these issues.

Thus we have employed UV spectroscopy to compare the states of protonation of dC residues in the third strand d(C-T)₆, when it binds to the target duplex d(A-G)₆·d(C-T)₆. Stretches of such duplex sequences are well known in eukaryotic genomes, particularly in promoter and gene switch regions, where they are thought to be prone to intramolecular triplex formation (H-DNA) (1,9). The approach taken depends on two considerations. One, when the third strand dissociates from the target strands well above the pK_a for dC, the nature of the accompanying spectral change will depend on whether or not the third strand dC residues in the triplex are protonated. This is because the spectra of neutral and protonated dC are markedly different, so that upon dissociation of the third strand the dC residues will lose a proton if bound by two H-bonds, but undergo no such large characteristic spectral change if held by just one H-bond. The second consideration stems from the fact that if the third strand dC residues are protonated at neutrality, then the stability of the triplex should show inverse dependence of stability on ionic strength.

The observations presented below are consistent with a two H-bond interaction at neutrality and above. Moreover, a thermodynamic analysis of the pH and ionic strength dependencies provides quantitative insights into the nature and properties of the C⁺:G·C base triplet. Finally, molecular modeling of the base triplets C:G·C, C⁺:G·C and T:A·T shows C⁺:G·C to be the most stable and the probability of formation of a C:G·C triplet with one H-bond to be extremely low, due to significant repulsion between the lone pairs on N7 of dG and N3 of dC in the third strand. These results imply that the limited availability of free protons within a cell can serve as a switch for binding of third strands with neutral residues that must be protonated in the triplex.

MATERIALS, METHODS AND THEORY

Samples

d(A-G)₆ and d(C-T)₆ were synthesized using standard phosphoramidite chemistry on an Applied Biosystems 380B synthesizer. The oligomers were purified by reverse phase HPLC (0.1 M triethylammonium acetate pH 7.0/acetone nitrile) and ion exchange HPLC (5 M urea/20 mM sodium phosphate pH 6.0, 5 M urea/20 mM sodium phosphate/1 M sodium sulfate pH 6.0) and desalted by reverse phase chromatography using C18 Sep-Pak. Purity was checked using reverse phase HPLC and PAGE on 16% denaturing gels after ³²P 5'-end labeling the oligomers, confirming their homogeneity. The purified oligomers were stored dry at -20°C. Molar extinction coefficients determined after phosphodiesterase I digestion ε₂₆₀ = 9890 for d(A-G)₆ and ε₂₆₀ = 8510 for d(C-T)₆ at 25°C in 2.6 × 10⁻⁵ M Tris pH 7.4/2.4 × 10⁻⁵ M MgCl₂, were used to determine oligomer concentration.

Unless otherwise stated, triplexes were prepared in a mixing buffer of 0.15 M NaCl/0.005 M MgCl₂/0.01 M cacodylate, titrated to the desired pH. Triplex mixtures were made with equimolar stocks of the two strands; after forming the duplex, a stoichiometric amount of the third strand was added.

UV spectroscopy and melting profiles

Absorption spectra and thermal melting profiles were determined in a computer driven AVIV 14DS spectrophotometer equipped with a thermoelectrically controlled holder. All samples were made with ddH₂O and degassed by bubbling helium through the solution. Filtered, dry air was passed through the cell compartment to prevent condensation on the cells at low temperatures. Flow rate was set low enough so as not to create a temperature gradient between the sample and the cell holder, which was confirmed by monitoring the temperature in the sample and cell holder during trial melting profiles. For melting experiments, spectral data were measured every 1 nm at 1°C intervals. Temperature was raised slowly enough to provide equilibrium melting profiles. T_m values obtained from the transition midpoint (α = 1/2) and from the maximum of the first derivative were the same. Sample integrity and hysteresis were checked by measuring each melting profile at least twice, with no significant differences observed (T_m ± 0.5°C).

The melting of duplex and triplex structures are each represented as a series of difference spectra between the spectrum at any temperature, T, and that at 1°C, projected in 3-D to make evident component transitions over a broad wavelength range. These 3-D melting representations were generated using AXUM 3.0 (18) and are plotted in Figure 1A-C, on the same scale, with wavelength every 1 nm (x-axis); temperature every 5°C (y-axis); absorbance difference (z-axis).

CD spectroscopy

CD spectra from 320 to 200 nm, every 0.2 nm (1 s average), with a 1.5 nm bandwidth were recorded at 1°C on a computer-driven AVIV 62DS CD spectrometer with a thermoelectrically controlled cell holder. The cell compartment was continuously purged with dry N₂. The data was smoothed by a least-squares polynomial fit of 7th order.

Molecular modeling

This was done on a PC (Intel 486DX, 33 MHZ, 16 MB RAM) with the program Amber as part of HyperChem (19). All parameters are those of Amber 3.0A (20), using the standard unmodified all-atom force field. For the protonated form of N1-methylcytosine, all the base charges are those of Amber 3.0A but for a proton on N3. Energy minimization of each base triplet alone, T:A·T, C⁺:G·C and C:G·C, with a methyl substituent at the glycosyl bond position of each base, was performed using a conjugate gradient method (Polak-Ribiere) and convergence was set at 0.1 kcal.Å⁻¹.mol⁻¹ for the rms gradient. No cutoff distance was used for non-bonded interactions and a distance dependent dielectric constant was used as a model solvent. No constraints were used in the energy minimizations.

Thermodynamic analysis of the triplex transition

The melting profile for the triplex shows two well resolved transitions corresponding to the dissociation of the third strand

from the core duplex, and for the melting of duplex at much higher temperature. Assuming there is no strand overlap at the low strand concentration at which the triplexes were formed (10^{-5} M), the transitions can be treated as separate intermolecular transitions; and because the strands are only 12 residues in size, each transition can be treated using a two-state analysis. This is consistent with the spectral data showing wavelength independence of T_m (Fig. 1A–F). The first transition, i.e., the dissociation of the third strand from the core duplex can be described by the equilibrium:



where, $T \equiv \text{triplex} = d(C^+-T)_6 \cdot [d(A-G)_6 \cdot d(C-T)_6]$; $D \equiv \text{duplex} = [d(A-G)_6 \cdot d(C-T)_6]$ and $S \equiv \text{single strand} = d(C-T)_6$.

If C_t is the total concentration of $D + S$ available to form T ; α is the fraction of third strand in triplex; D and S are each always present at the same concentration $(1 - \alpha) \frac{C_t}{2}$; and $(\alpha) \frac{C_t}{2}$ is the concentration of T ; then the observed equilibrium constant is

$$K_{obs} = \frac{[D][S]}{[T]} = \frac{(1-\alpha)^2 \frac{C_t}{2}}{\alpha} \quad \text{with } \alpha = \frac{A(\text{duplex+coil})_{255} - A_{255}}{A(\text{duplex+coil})_{255} - A(\text{triplex})_{255}} \quad 1$$

where K_{obs} is obtained from the equilibrium between the triplex and the core duplex + third strand, in contrast to K_{expl} that explicitly includes Na^+ and H^+ in the equilibrium (see below); the hyperchromic change at 255 nm is a measure of the dissociation of triplex; $A(\text{triplex})_{255}$ is the absorbance of intact triplex; $A(\text{duplex + coil})_{255}$ is the sum of the absorbances of duplex and single strand; A_{255} is the absorbance at any temperature within the transition.

Values for the observed van't Hoff enthalpy for the transition, ΔH°_{obs} , were obtained according to 2, from a plot of $\ln K_{obs}$ vs $1/T$

$$\ln K_{obs} = \frac{-\Delta H^{\circ}_{obs}}{RT} + \frac{\Delta S^{\circ}_{obs}}{R} \quad 2$$

where R is the gas constant ($1.989 \text{ cal} \cdot \text{K}^{-1} \cdot \text{mol}^{-1}$) and T is the absolute temperature interval over which the transition occurs.

The value for the observed transition entropy, ΔS°_{obs} , was then calculated at $T = T_m$. Values for the observed transition free energy at 25°C , ΔG°_{obs} , were obtained from

$$\Delta G^{\circ}_{obs} = \Delta H^{\circ}_{obs} \left(1 - \frac{T_{298}}{T_m}\right) \quad 3$$

To evaluate the effects of the ionic environment on triplex stability, both electrostatic shielding (Debye–Hückel) by the counterion atmosphere and condensation of counterions (Na^+) onto the nucleic acid polyelectrolyte are considered. To these are added site binding of H^+ on a ring N of a base, which may be viewed as a special type of condensation. This analysis assumes the site binding of the H^+ ions bound to N3 of the third strand dC residues in the triplex can be treated in a manner comparable to that used for condensed Na^+ ions, which seems justified because those H^+ ions reduce the net negative charge in the triplex structure, thereby effectively reducing the amount of Na^+ condensation. This approach is supported by the observed inverse ionic strength dependence of triplex stability, and as seen below, gives a chemically meaningful value for the number of protons bound by the third strand in the triplex.

Following Manning's approach (21,22), let Z be the negative charge per phosphate separated by their average spacing b . Then, the extent of counter ion binding is given by the dimensionless parameter

$$\xi = \frac{e^2}{b\epsilon kT} \quad 4$$

where e is the charge of the electron, ϵ is the solvent dielectric constant, k is the Boltzmann constant and T is the absolute temperature. [Our duplex and triplex length is $\approx 41 \text{ \AA}$ ($3.4 \text{ \AA} \times 12$) which, for the ionic strengths studied here, is longer than the Debye length, κ^{-1} . Using 7 and 8: $\kappa^{-1} = 1.7 \text{ \AA}$ (3 M NaCl solution); 7.3 \AA (mixing buffer solution); 9.1 \AA (0.1 M NaCl solution).]

The fraction of counterion condensation per charge

$$\theta_m = 1 - \frac{1}{\xi} \quad 5$$

That is, after counterion condensation, a net negative charge of $1 - \theta_m$ remains on each phosphate and must be screened by the counterion atmosphere. Using a shielded potential, the electrostatic free energy per mole of phosphate associated with counterion screening

$$G_{el} = -RT \frac{1}{\xi} \ln \kappa b \quad 6$$

where the Debye–Hückel screening parameter for a cylindrical geometry

$$\kappa = \left(\frac{4\pi e^2}{\epsilon kT} \right)^{1/2} I^{1/2} \quad 7$$

and the ionic strength of the solution

$$I = \sum_i \frac{C_i z_i^2}{2} \quad 8$$

where C_i is the molar concentration of the i th counterion species with charge z_i .

Having developed a general form of the electrostatics, we now explicitly introduce Na^+ and H^+ into the equilibrium for the dissociation of triplex to duplex and third strand, thus:



where Δn_1 is the number of Na^+ released or bound, Δn_2 is the number of H^+ released or bound, and T , D and S are triplex, duplex and single strand, respectively.

The explicit Gibbs free energy change associated with release of third strand, ΔG_{expl} , has the following components: $\Delta G_{structure}$, the change associated with separation of third strand and duplex (i.e., ΔH due to loss or gain of H-bonding and base stacking, ΔS due to loss or gain of conformational and vibrational freedom of the system); ΔG_{Na^+} , the change associated with release or uptake of Na^+ ; ΔG_{H^+} , the change associated with release or uptake of H^+ ; $\Delta G_{el Na^+}$, the change associated with the different ion-atmosphere shielding by Na^+ of the triplex versus duplex plus single strand; $\Delta G_{el H^+}$, the change associated with the different ion-atmosphere shielding of the triplex versus duplex plus single strand for H^+ . Since only the triplex contains H^+ ions, this effect comes from their contribution to electrostatic shielding by way of reducing the net charge on the triplex.

For completeness, a sixth free energy change associated with the difference in water binding or hydration of the triplex versus that of the duplex plus single strand should be included. However, we do not address the water explicitly and this factor is considered as part of ΔG° .

For a triplex with Z_1 phosphates, the change in the number of condensed Na^+ on dissociation of the third strand is

$$\Delta n_1 = n_{1T} - n_{1D} - n_{1S} = Z_1 \left(1 \left[1 - \frac{1}{\xi(T)} \right] - \frac{2}{3} \left[1 - \frac{1}{\xi(D)} \right] - \frac{1}{3} \left[1 - \frac{1}{\xi(S)} \right] \right) = Z_1 \left(\frac{2}{3\xi(D)} + \frac{1}{3\xi(S)} - \frac{1}{\xi(T)} \right) \quad 10$$

where n_{1T} is the average number of Na^+ bound to triplex; n_{1D} is the average number of Na^+ bound to duplex; n_{1S} is the average number of Na^+ bound to single strand.

Knowing that Na^+ and H^+ must both contribute to electrostatic shielding of the triplex, we use the Debye-Hückel approximation for a shielded potential and obtain expressions for the Na^+ and H^+ dependence.

For a solution with Na^+ concentration M_1 , the entropic contribution of the Na^+ counterions to the free energy of third strand dissociation

$$\Delta G_{\text{Na}^+} = -RT Z_1 \left(\frac{2}{3\xi(D)} + \frac{1}{3\xi(S)} - \frac{1}{\xi(T)} \right) \ln[M_1] = -RT \Delta n_1 \ln[M_1] \quad 11$$

and for a triplex with Z_1 phosphates, using 6, the shielding contribution (enthalpic contribution) of the Na^+ counterions to the free energy of third strand dissociation

$$\Delta G_{\text{el Na}^+} = -RT Z_1 \left\{ \left[\frac{1}{\xi(T)} \ln \kappa b_{(T)} \right] - \left[\frac{2}{3\xi(D)} \ln \kappa b_{(D)} \right] - \left[\frac{1}{3\xi(S)} \ln \kappa b_{(S)} \right] \right\}. \quad 12$$

Assuming the fraction of H^+ bound per third strand dC residue to be given by $1 - \frac{1}{\xi}$, and that their contribution to the electrostatic shielding can be modeled by a shielded potential, then the H^+ contribution to the free energy of third strand dissociation has the following entropic 14 and enthalpic 15 components, with the change in the number of H^+ on third strand dissociation, Δn_2 , given by:

$$\Delta n_2 = n_{2T} - n_{2S} = Z_2 \left(1 \left[1 - \frac{1}{\xi(T)} \right] - 1 \left[1 - \frac{1}{\xi(S)} \right] \right) = Z_2 \left(\frac{1}{\xi(S)} - \frac{1}{\xi(T)} \right) \quad 13$$

where n_{2T} is the average number of H^+ site bound to triplex; n_{2S} is the average number of H^+ site bound to single strand; and Z_2 is the total number of potential H^+ binding sites in the triplex. [For both Na^+ and H^+ binding, $\frac{1}{\xi}$ must be dependent on the phosphate and third strand dC residue spacing. Equations 21 and 23 are still valid if the fraction of H^+ bound per third strand dC residue, θ_{H^+} , is not described by $1 - \frac{1}{\xi}$, but some other unknown function, $1 - \text{fnc}$. That is,

$$\frac{\partial T_m}{\partial (\ln[\text{H}^+])} = \frac{1}{2} \frac{\Delta n_2 R (T_m)^2}{Z_2 \Delta H_2} \text{ and } \Delta n_2 = Z_2 (\text{fnc}_{(S)} - \text{fnc}_{(T)}).$$

Then, for a solution with H^+ concentration M_2 , the entropic contribution of the bound H^+ to the free energy of third strand dissociation

$$\Delta G_{\text{H}^+} = -RT Z_2 \left(\frac{1}{\xi(S)} - \frac{1}{\xi(T)} \right) \ln[M_2] = -RT \Delta n_2 \ln[M_2] \quad 14$$

and for a triplex with protonated dC residues, from 6, the shielding contribution (enthalpic contribution) to the free energy of third strand dissociation

$$\Delta G_{\text{el H}^+} = -RT Z_2 \left\{ \left[\frac{1}{\xi(T)} \ln \kappa b_{(T)} \right] - \left[\frac{1}{\xi(S)} \ln \kappa b_{(S)} \right] \right\}. \quad 15$$

Substituting 11, 12, 14 and 15 into

$$\Delta G_{\text{expl}} = (\Delta G_{\text{structure}}) + (\Delta G_{\text{Na}^+}) + (\Delta G_{\text{el Na}^+}) + (\Delta G_{\text{H}^+}) + (\Delta G_{\text{el H}^+})$$

and using $\ln K_{\text{expl}} = \frac{-\Delta G_{\text{expl}}}{RT}$ we obtain

$$\begin{aligned} \ln K_{\text{expl}} = & \ln K_{\text{structure}} + Z_1 \left(\frac{2}{3\xi(D)} + \frac{1}{3\xi(S)} - \frac{1}{\xi(T)} \right) \ln[M_1] \\ & + Z_1 \left\{ \left[\frac{1}{\xi(T)} \ln \kappa b_{(T)} \right] - \left[\frac{2}{3\xi(D)} \ln \kappa b_{(D)} \right] - \left[\frac{1}{3\xi(S)} \ln \kappa b_{(S)} \right] \right\} \\ & + Z_2 \left(\frac{1}{\xi(S)} - \frac{1}{\xi(T)} \right) \ln[M_2] + Z_2 \left\{ \left[\frac{1}{\xi(T)} \ln \kappa b_{(T)} \right] - \left[\frac{1}{\xi(S)} \ln \kappa b_{(S)} \right] \right\}. \end{aligned} \quad 16a$$

For a monovalent electrolyte, $\kappa = \left(\frac{4\pi e^2}{\epsilon kT} \right)^{1/2} [M]^{1/2} = \kappa' [M]^{1/2}$.

Substituting for κ and simplifying, we obtain

$$\begin{aligned} \ln K_{\text{expl}} = & \ln K_{\text{structure}} + \frac{1}{2} Z_1 \left(\frac{2}{3\xi(D)} + \frac{1}{3\xi(S)} - \frac{1}{\xi(T)} \right) \ln[M_1] \\ & + Z_1 \frac{1}{\xi(T)} \ln \kappa' b_{(T)} - Z_1 \frac{2}{3\xi(D)} \ln \kappa' b_{(D)} - Z_1 \frac{1}{3\xi(S)} \ln \kappa' b_{(S)} \\ & + \frac{1}{2} Z_2 \left(\frac{1}{\xi(S)} - \frac{1}{\xi(T)} \right) \ln[M_2] + Z_2 \frac{1}{\xi(T)} \ln \kappa' b_{(T)} - Z_2 \frac{1}{\xi(S)} \ln \kappa' b_{(S)}. \end{aligned} \quad 16b$$

Thus, the effect of Na^+ concentration (M_1) on the explicit equilibrium constant is

$$\frac{\partial (\ln K_{\text{expl}})}{\partial (\ln [\text{Na}^+])} = \frac{1}{2} Z_1 \left(\frac{2}{3\xi(D)} + \frac{1}{3\xi(S)} - \frac{1}{\xi(T)} \right) = \frac{1}{2} \Delta n_1 \quad 17$$

and the effect of H^+ concentration (M_2) on the explicit equilibrium constant is

$$\frac{\partial (\ln K_{\text{expl}})}{\partial (\ln [\text{H}^+])} = \frac{1}{2} Z_2 \left(\frac{1}{\xi(S)} - \frac{1}{\xi(T)} \right) = \frac{1}{2} \Delta n_2. \quad 18$$

The temperature dependence of $\ln K_{\text{expl}}$ is

$$\frac{\partial (\ln K_{\text{expl}})}{\partial T} = \frac{\partial}{\partial T} \left(\frac{-\Delta G}{RT} \right) = \frac{\Delta H}{RT^2}. \quad 19$$

Finally, we obtain expressions giving the effect of counterion concentration on triplex stability, as reflected by observed T_m values. Thus

$$\frac{\partial T_m}{\partial (\ln[\text{Na}^+])} = \frac{\partial (\ln K_{\text{expl}})}{\partial (\ln[\text{Na}^+])} \times \frac{\partial T_m}{\partial (\ln K_{\text{expl}})} = \frac{1}{2} \frac{\Delta n_1 R (T_m)^2}{Z_1 \Delta H_1} \quad 20$$

$$\frac{\partial T_m}{\partial (\ln[\text{H}^+])} = \frac{\partial (\ln K_{\text{expl}})}{\partial (\ln[\text{H}^+])} \times \frac{\partial T_m}{\partial (\ln K_{\text{expl}})} = \frac{1}{2} \frac{\Delta n_2 R (T_m)^2}{Z_2 \Delta H_2} \quad 21$$

Integration and simplification of 20 and 21 yields respectively

$$\Delta \left[\frac{1}{T_m} \right] = -\frac{1}{2} \left(\frac{2}{3\xi(D)} + \frac{1}{3\xi(S)} - \frac{1}{\xi(T)} \right) \frac{2.303R}{\Delta H_1} \Delta (\log[\text{Na}^+]) \quad 22$$

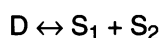
$$\Delta\left[\frac{1}{T_m}\right] = -\frac{1}{2}\left(\frac{1}{\xi_{(S)}} - \frac{1}{\xi_{(T)}}\right)\frac{2.303R}{\Delta H_2}\Delta(-pH) \quad 23$$

where $\frac{\Delta n_1}{Z_1}$ is the stoichiometric change in Na^+ bound per phosphate; ΔH_1 is the enthalpy change per mole phosphate; Δn_1 is the stoichiometric change in Na^+ bound on triplex dissociation, and $\frac{\Delta n_2}{Z_2}$ is the stoichiometric change in H^+ bound per third strand dC residue; ΔH_2 is the enthalpy change per mole third strand dC residue; Δn_2 is the stoichiometric change in H^+ bound on triplex dissociation.

While Manning's approach to include ionization of the nucleic acid bases and the effect that this has on the Na^+ and H^+ dependence has previously been extended by Record *et al.* (23), there are distinct differences between their results and ours (see Discussion).

Thermodynamic analysis of the duplex transition

The melting of the duplex in both the duplex and triplex mixtures is described by the following equilibrium:



where $D \equiv \text{duplex} = d(\text{A-G})_6 \cdot d(\text{C-T})_6$; $S_1 \equiv \text{single strand} = d(\text{C-T})_6$ and $S_2 \equiv \text{single strand} = d(\text{A-G})_6$.

For these non-self complementary strands, the observed equilibrium constant

$$K_{obs} = \frac{[S_1][S_2]}{[D]} = \frac{(1-\alpha)^2 C_1}{\alpha} \quad 24$$

for the duplex mixture,

$$\text{with } \alpha = \frac{A(\text{coil})_{255} - A_{255}}{A(\text{coil})_{255} - A(\text{duplex})_{255}}$$

while for the triplex mixture,

$$K_{obs} = \frac{2[S_1][S_2]}{[D]} = \frac{(1-\alpha)^2 \frac{2C_1}{3}}{\alpha} \quad 25$$

$$\text{with } \alpha = \frac{A(\text{coil})_{255} - A_{255}}{A(\text{coil})_{255} - A(\text{duplex} + \text{coil})_{255}}$$

where α is the fraction of single strand in duplex; and C_1 is the total concentration of single strands. The fraction of dissociated duplex is measured in terms of the quantities $A(\text{duplex})_{255}$, the absorbance of the duplex; $A(\text{coil})_{255}$, the absorbance of the separated strands; A_{255} , the absorbance at some temperature within the transition; and $A(\text{duplex} + \text{coil})_{255}$, the absorbance of the duplex and dissociated single strand.

RESULTS

Identifying the triplex and duplex transitions

Melting of the triplex formed from $d(\text{C-T})_6$ and $[d(\text{A-G})_6 \cdot d(\text{C-T})_6]$ at pH 7.0, is shown in Figure 1B, where the absorbance difference spectrum ($\Delta A_\lambda = \Delta \epsilon \text{CL}$) over a range of wavelengths, λ , at any temperature, T , is given by $\Delta A_{\lambda,T}$ (triplex mixture) = $A_{\lambda,T} - A_{\lambda,1^\circ}$. Two transitions are apparent, one between 5 and 15°C and the second between 40 and 60°C. The

first transition must represent dissociation of the third strand from the core duplex of the triplex since the second transition clearly coincides with that for the duplex alone at the same pH (Fig. 1A). Similarly, Figure 1C shows the comparable melting pattern of the triplex at pH 4.2, with the first transition occurring from 25 to 35°C and the second from 55 to 70°C.

Melting profiles at individual wavelengths between 240 and 280 nm for the duplex mixture at pH 7.0 (e.g., Fig. 1D) and the triplex mixture at pH 7.0 (e.g., Fig. 1E) and pH 4.2 (e.g., Fig. 1F), clearly illustrate the features of the thermal transition(s) and confirm that T_m is wavelength independent. This behavior is consistent with cooperative transition(s) as all the chromophores undergo spectral changes simultaneously.

An analysis of the difference in spectral changes on triplex melting at the two pH values is given below; so is a thermodynamic analysis of the pH dependence of T_m for the transition.

Spectroscopic characterization of the triplex→duplex transition

Of the four residues contained in the triplex, only dC shows significant near-UV spectral differences under relevant acidic and neutral conditions. On dissociating a proton from 5'dC⁺MP (pK_a 4.6), these differences take the form of a positive peak between 220 and 265 nm and a negative peak centered at 288 nm (Fig. 2A). Hoogsteen pairing of a third strand dC residue to the dG residue of a target G·C base pair results in a base triplet that is isostructural to T:A·T (Fig. 9), the third strand dC residue interacting with the target dG via two H-bonds if it is protonated at N3 (Fig. 10), and via one H-bond if it is not. Moreover, if the third strand dC residues are protonated at all pH values where the triplex exists, the fraction that should lose their protons on third strand dissociation at any given pH can be estimated by assuming that the pK_a of dC in $d(\text{C}^+-\text{T})_6$ is the same as for dCMP, i.e., 28% at pH 4.2 and 100% at pH 7.0. This means that at pH 4.2 the characteristic spectral change for $d\text{C}^+ \rightarrow d\text{C}$ should contribute to the total spectral change upon third strand dissociation from the core duplex only to a small extent, whereas at pH 7.0 the contribution should be very pronounced. We have therefore particularly evaluated the observed spectral change on third strand dissociation for evidence of that characteristic contribution for $d\text{C}^+ \rightarrow d\text{C}$ at pH 7.0.

To do so we ask whether the total spectral change, ΔA_λ , observed on dissociating the putative third strand $d(\text{C}^+-\text{T})_6$ from the core duplex $d(\text{A-G})_6 \cdot d(\text{C-T})_6$ at pH 7.0 is a linear combination of the following 'library' spectral contributions: (i) the dissociation and unstacking of dT from A·T target base pairs ($\Delta A_\lambda, \text{T:A}\cdot\text{T} \rightarrow \text{T} + \text{A}\cdot\text{T}$); (ii) the dissociation and unstacking of dC⁺ from G·C target base pairs ($\Delta A_\lambda, \text{C}^+:\text{G}\cdot\text{C} \rightarrow \text{C}^+ + \text{G}\cdot\text{C}$); (iii) the consecutive deprotonation of dC⁺ \rightarrow dC at pH 7.0 ($\Delta A_\lambda, \text{C}^+ \rightarrow \text{C}$).

The first spectral library component, $\Delta A_\lambda, \text{T:A}\cdot\text{T} \rightarrow \text{T} + \text{A}\cdot\text{T}$, was obtained from the difference spectrum [(duplex + single strand) - (triplex)] for the dissociation of the third strand (dT)₂₁ from the core duplex (dA)₂₁·(dT)₂₁ in neutral mixing buffer. That difference spectrum (Fig. 2B) shows a broad peak centered at 265 nm.

The second spectral library component, $\Delta A_\lambda, \text{C}^+:\text{G}\cdot\text{C} \rightarrow \text{C}^+ + \text{G}\cdot\text{C}$, was approximated from the difference spectrum [(poly(dC), 80°C) - (poly(dC), 1°C)], i.e., for the melting of poly(dC) in neutral mixing buffer. This component (Fig. 2C) shows the

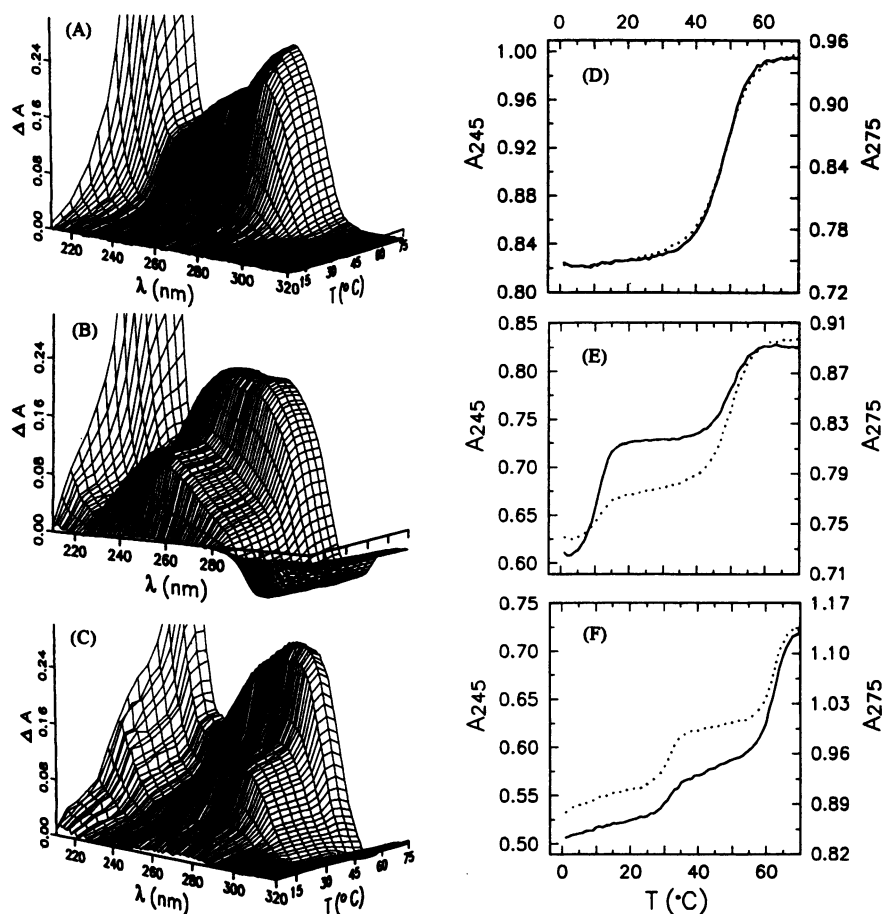


Figure 1. (A) Melting spectra, $\Delta A_{\lambda,T}$ (duplex mixture) = $A_{\lambda,T}$ (duplex mixture) - $A_{\lambda,1^\circ}$ (duplex mixture), of duplex mixture in mixing buffer at pH 7.0. The scan at 1°C was subtracted from all subsequent scans, so the plot represents a series of temperature dependent difference spectra. (B) Melting spectra, $\Delta A_{\lambda,T}$ (triplex mixture) = $A_{\lambda,T}$ (triplex mixture) - $A_{\lambda,1^\circ}$ (triplex mixture), of triplex mixture in mixing buffer at pH 7.0 [y-axis labels omitted for clarity]. (C) Melting spectra, $\Delta A_{\lambda,T}$ (triplex mixture) = $A_{\lambda,T}$ (triplex mixture) - $A_{\lambda,1^\circ}$ (triplex mixture), of triplex mixture in mixing buffer at pH 4.2. (D) Melting profiles of duplex mixture in mixing buffer at pH 7.0, measured at 245 nm (—) and 275 nm (· · ·). T_m is wavelength independent, consistent with a cooperative transition. (E) Melting profiles of triplex mixture in mixing buffer at pH 7.0, measured at 245 nm (—) and 275 nm (· · ·). T_m values are wavelength independent for both transitions. (F) Melting profiles of triplex mixture in mixing buffer at pH 4.2, measured at 245 nm (—) and 275 nm (· · ·). T_m values are wavelength independent for both transitions.

double peak characteristic of unstacking dC residues, and its use implies that it is very similar for unstacking dC⁺ residues.

The third spectral library component, $\Delta A_{\lambda, C^+ \rightarrow C}$, was obtained from dCMP, pH 7.0 - dC⁺MP, pH 2.0 in 0.05 M sodium phosphate buffer at 25 °C, as described above (Fig. 2A). The sum of the three library spectra is shown in Figure 2D along with the observed difference spectrum for third strand dissociation at pH 7.0. While the two spectra do not coincide, it can be seen that they do so when the summated one is displaced on the wavelength axis +6 nm, as can be seen in Figure 2E. That the sum of the library spectra needs to be red shifted 6 nm is not unreasonable given that the library spectra do not account for the characteristic red shift that occurs on breaking H-bonds between bases (24), in this case between the third strand dC⁺ residues and the target dG residues. Moreover, the second spectral library component accounts for the unstacking of dC rather than dC⁺ residues, the latter being inaccessible because poly(dC⁺) forms a hemiprotonated double stranded helix under acidic conditions (25,26). These two limitations notwithstanding, it is apparent that the spectral components contributing to third strand dissociation from the

duplex are quite well approximated, and that the major contribution to the difference spectrum at pH 7.0 derives from deprotonation of the third strand dC⁺ residues. That being the case, the third strand dC residues must be fully protonated in the triplex.

Figure 3 shows difference spectra for third strand dissociation as a function of pH. The reason for the large blue shift as pH rises is that the library component for dC⁺ → dC (Fig. 2A) makes an increasingly greater contribution, resulting in increasing enhancement of the peak at 245 nm and the trough at 294 nm, while the contribution from the two other spectral components is unchanging. At pH 4.2, for example, the difference spectrum shows a broad peak centered at 275 nm due to the dissociation and unstacking of the dT residues from the A · T target base pairs. That peak is seen only as a shoulder of the main peak at pH 5.0 and 7.0, due to the superposition of the large contribution of the dC⁺ → dC difference spectrum.

In sum, UV spectroscopic evidence shows that at pH 7.0 the third strand dC residues are protonated in the triplex and therefore the presence of two H-bonds in the Hoogsteen C⁺:G base pair component. If the Hoogsteen pair of the C:G · C base triplet could

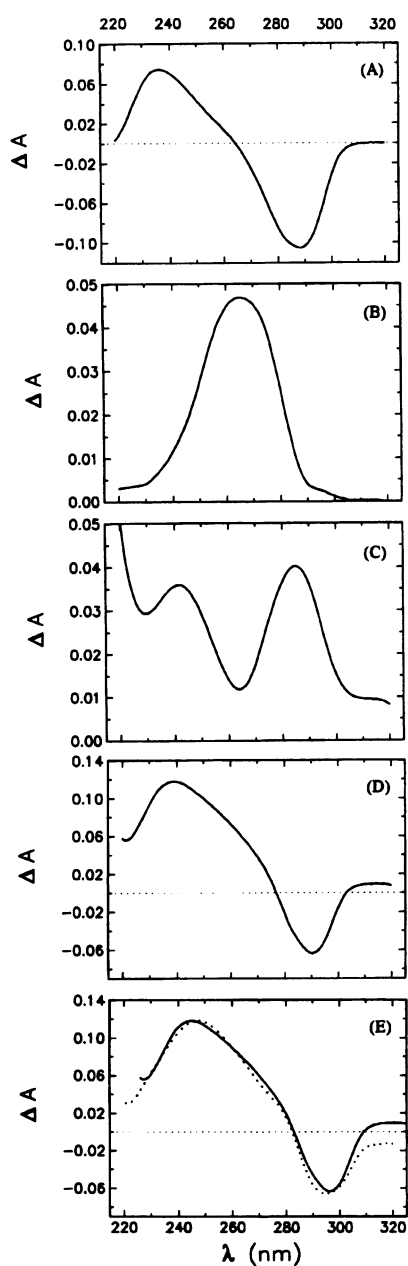


Figure 2. Library spectral components for analysis of dissociation of the triplex at different pH values. (A) Spectral change associated with deprotonation of dC^+MP , i.e., $\Delta A = A_{\lambda, \text{pH } 7.0} - A_{\lambda, \text{pH } 2.0}$ in 0.05 M sodium phosphate buffer at 25°C. This is taken to represent the spectral change associated with deprotonation of dC^+ residues in the third strand, i.e., $\Delta A_{\lambda, C^+ \rightarrow C}$. (B) Spectral change associated with both dissociation and unstacking of dT residues from A·T target base pairs ($\Delta A_{\lambda, T:A \cdot T \rightarrow T + A \cdot T$). It was obtained from the difference spectrum [(duplex + melted single strand) - (triplex)] for the dissociation of the third strand $(dT)_{21}$ from the core duplex $(dA)_{21} \cdot (dT)_{21}$ in neutral mixing buffer. (C) Spectral change associated with unstacking of dC residues from poly(dC), i.e., $\Delta A_{\lambda, 80-1^\circ C}$, in neutral mixing buffer. This difference spectrum was used to mimic the change due to unstacking of third strand dC^+ residues upon dissociation from G·C target base pairs ($\Delta A_{\lambda, C^+ \cdot G \cdot C \rightarrow C^+ + G \cdot C$). (D) Spectral change calculated for the dissociation at pH 7.0 of $d(C-T)_6$ from the target duplex by linear summation of the difference spectra in (A), (B) and (C). (E) Comparison of the calculated difference spectrum in (D), displaced +6 nm (—), with the melting difference spectrum (20–1°C) of the triplex at pH 7.0 (···).

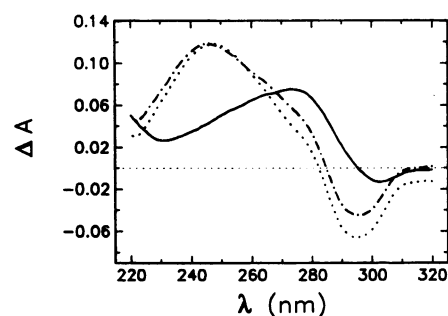
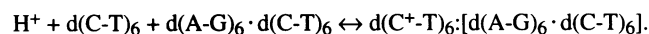


Figure 3. Difference spectra (20–1°C) for the triplex mixture at pH 4.2 (—), 5.0 (---) and 7.0 (···) in mixing buffer.

form with only one H-bond, then that pair should remain stable so long as the target base pair is stable. Yet, the hyperchromic change at 255 nm on dissociating the third strand drops from 12% at both pH 5.0 and pH 7.0 to 4% at pH 7.5. This 2/3 loss of hyperchromic change indicates a comparably reduced proportion of triplex formation, a reduction which can be ascribed to the limited availability of H^+ ions, which are required to drive the equilibrium toward triplex formation, thus:



In this respect, hydrogen ion concentration may be seen as a switch for triplex formation.

Thermodynamic parameters for the triplex and duplex transitions

It is evident from the linearity of the van't Hoff plots in Figures 4, 5 and 6 that the data obtained from the UV melting profiles are in accord with that type of analysis, i.e., the enthalpy change over the temperature range of each transition is essentially constant. This enables the accumulation of the standard molar thermodynamic parameters given in Table 1. The average ΔH°_{obs} per mole base pair were obtained by dividing ΔH°_{obs} per mole oligomer by 12, the number of residues per strand that are unstacking in the transition. This analysis was possible as the transitions are well separated, cooperative and have good baselines. The one exception to this were the triplex and duplex profiles at pH 4.2, which had poor baselines and gave anomalously high enthalpy values.

The unique occurrence of high T_m values for the duplex at pH 4.2 in both the duplex (57°C) and triplex (62°C) mixtures suggested the presence of some species other than a Watson-Crick duplex (48°C). Since protonation of dC at N_3 must lead to disruption of a Watson-Crick G·C base pair, and both protonated dC and neutral dT residues are amenable to isostructural Hoogsteen pairing with dG and dA respectively, we inferred that at low pH $d(C^+-T)_6 + d(A-G)_6$ must form a parallel Hoogsteen rather than an antiparallel Watson-Crick duplex. In fact, such a duplex has been observed at low pH (27) for a similar 20mer sequence. The CD spectra of this duplex at pH 4.2 and 7.0 (Fig. 10), in comparison with those in (27), confirm the formation of a parallel Hoogsteen duplex under acidic conditions.

The enthalpy values show that under all conditions studied the Hoogsteen-bound third strand in the triplex is more tightly held than the comparable Watson-Crick strand (in the duplex). For

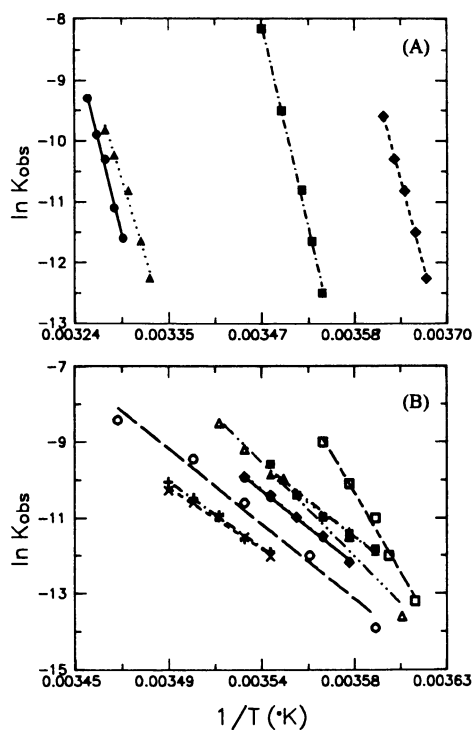


Figure 4. van't Hoff plots for the first transition of triplex mixtures (triplex dissociation to third strand + duplex). (A) mixing buffer, pH 4.2 (●), 5.0 (▲), 7.0 (■), 7.5 (◆). (B) 0.01 M cacodylate pH 7.0, with 0.1 M NaCl (●), 0.3 M NaCl (▲), 0.4 M NaCl (■), 0.5 M NaCl (◆), 0.8 M NaCl (+), 0.9 M NaCl (x), 1.0 M NaCl (o), 2.0 M NaCl (Δ), 3.0 M NaCl (□).

example, at pH 7.0 in mixing buffer, $\Delta H^{\circ}_{obs} = 6.4 \text{ kcal.mol}^{-1}$ base pair for duplex dissociation, and $9.7 \text{ kcal.mol}^{-1}$ base pair for third strand dissociation. In addition, the formation of a parallel Hoogsteen duplex at pH 4.2 with 11 base pair interactions and a significantly higher T_m than that of the Watson-Crick duplex with 12 base pair interactions clearly confirms the greater stability of the Hoogsteen interactions. This finding is consistent with several earlier observations: (i) Hoogsteen (28) found that 1-methylthymine and 9-methyladenine co-crystallize only in an H-bonding geometry that is different ('Hoogsteen') from that of the Watson-Crick A·T base pair. (ii) Ornstein and Fresco (29) calculated that the Hoogsteen T:A base pair is more stable by $-1.03 \text{ kcal.mol}^{-1}$ than the Watson-Crick A·T base pair. (iii) In contrast, the monomers of C and G only co-crystallize in the Watson-Crick G·C geometry, and not in the neutral Hoogsteen C:G geometry. (iv) The total H-bond interaction energy for a neutral H-bond consists of dispersion, polarization and electrostatic components, with the latter contributing about 80% of the total energy. Hence, for the Hoogsteen C⁺:G base pair with an ionic H-bond, the interaction energy is higher. In fact, doubling and tripling of the interaction energy for ionic H-bonds has been both calculated and experimentally observed (30,31). Further, Pullman *et al.* (32) calculated interaction energies (kcal.mol^{-1}) for base pairs and triplets as follows: UAU -12, Watson-Crick GC -19, Hoogsteen CC +13, Hoogsteen C⁺C -35, C⁺GC -48, with the latter triplet the most stable.

The foregoing trends in the enthalpy values notwithstanding, under all conditions studied, the free energy of formation of

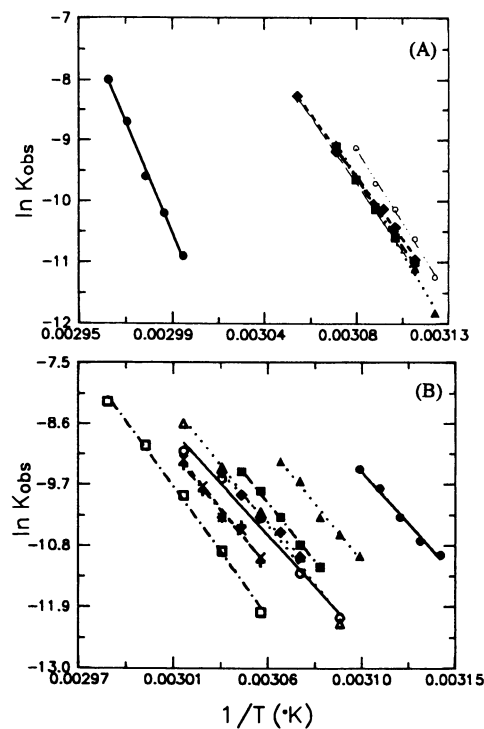


Figure 5. van't Hoff plots for the second transition of triplex mixtures (duplex dissociation in presence of the third strand). (A) mixing buffer, pH 4.2 (●), 5.0 (▲), 7.0 (■), 7.5 (◆), 8.0 (+), 8.5 (x). The plots superimpose between pH 5.0 and 8.5, indicating that T_m for the duplex is pH independent over this range. (B) 0.01 M cacodylate pH 7.0, with 0.1 M NaCl (●), 0.3 M NaCl (▲), 0.4 M NaCl (■), 0.5 M NaCl (◆), 0.8 M NaCl (+), 0.9 M NaCl (x), 1.0 M NaCl (o), 2.0 M NaCl (Δ), 3.0 M NaCl (□).

triplex at 25°C is less than that for the comparable Watson-Crick duplex. For example, at pH 7.0 in mixing buffer, $\Delta G^{\circ}_{obs,298} = -5.5 \text{ kcal.mol}^{-1}$ oligomer for duplex formation but $5.7 \text{ kcal.mol}^{-1}$ oligomer for triplex formation. The less favorable free energy values for formation of the triplex obviously result from their more negative ΔS°_{obs} values than those for the duplex under comparable conditions (Table 1). Thus, for this triplex, association of the third strand to the duplex is enthalpically driven (favorable) and entropically unfavorable. This behavior is consistent with proton uptake by the third strand dC residues.

For triplex formation the free energy at 25°C becomes increasingly negative with decreasing pH, as is expected with the requirement that third strand dC residues be protonated ($\Delta G^{\circ}_{obs,298} = 8.5 \text{ kcal.mol}^{-1}$ oligomer at pH 7.5, 5.7 at pH 7.0, -1.2 at pH 5.0, and -2.5 at pH 4.2 (Table 1). Finally, the endergonic values at pH 7.0 and 7.5 are consistent with the fact that the triplex does not exist at 25°C , its T_m values under these conditions being 11 and 1°C , respectively.

The high values of ΔH°_{obs} , ΔS°_{obs} and ΔG°_{obs} for the triplex in 3 M NaCl merit additional comment. The large positive ΔH°_{obs} of $15.4 \text{ kcal.mol}^{-1}$ base pair dissociation shows the third strand binding interactions to be favorable. At the same time, the large positive ΔS°_{obs} ($0.67 \text{ kcal.mol}^{-1}\cdot\text{K}^{-1}$ oligomer) is significant in that it compensates for this positive enthalpy change, resulting in a negative ΔG°_{obs} ($-13.3 \text{ kcal.mol}^{-1}$ oligomer). The significantly larger ΔS°_{obs} for dissociation of third strand at 3 M NaCl must to

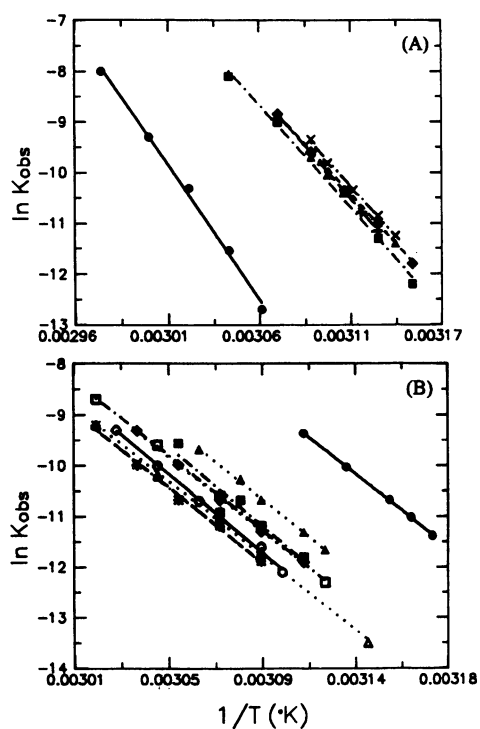


Figure 6. van't Hoff plots for melting of duplex. (A) mixing buffer, pH 4.2 (●), 5.0 (▲), 7.0 (■), 7.5 (◆), 8.0 (+), 8.5 (x). The plots superimpose between pH 5.0 and 8.5, indicating that T_m for the duplex is pH independent over this range. (B) 0.01 M cacodylate pH 7.0, with 0.1 M NaCl (●), 0.3 M NaCl (▲), 0.4 M NaCl (■), 0.5 M NaCl (◆), 0.8 M NaCl (+), 0.9 M NaCl (x), 1.0 M NaCl (o), 2.0 M NaCl (Δ), 3.0 M NaCl (□).

a significant extent result from an increase in entropy of the water, as the dissociated duplex and single strand have a net gain of 9 Na^+ (see next section). That is, removal of ions from the solution results in the release of H_2O from the ion- H_2O clusters that were in solution. This is also the case for 2 M NaCl (5 Na^+) and 1 M NaCl (4 Na^+), but to a lesser extent. We note also that the percent hyperchromicity for the third strand dissociation is significantly less in 3 M NaCl: 1.0 M NaCl 17%; 2 M NaCl 13%; 3 M NaCl 2%. This significant reduction in the percent hyperchromicity is probably due to the equilibrium being shifted to the right, resulting in less triplex formation under these conditions and therefore an anomalous value of $\Delta H^{\circ}_{\text{obs}}$ for the triplex in 3 M NaCl.

Sodium ion dependence of third strand binding

The thermal stability of the triplex is not affected on increasing NaCl concentration from 0.1 to 0.4 M, but above 0.4 M increases to a maximum at ~ 0.9 M ($T_m = 10^\circ\text{C}$) and then decreases to 5°C at 3 M NaCl (Table 1 and Fig. 7A–C). That decreasing NaCl concentration < 0.4 M has no effect on T_m was repeatedly confirmed. This unusual behavior must result from the protons of dC^+ contributing to the stability of the triplex. That this is not an artifactual result is shown by the T_m for the duplex in the triplex solution decreasing in the normal manner below 0.4 M. Thus, Figure 7C shows the $\log[\text{NaCl}]$ dependence for the duplex in triplex solution and for the duplex in duplex solution, confirming the decreasing ionic strength of these solutions.

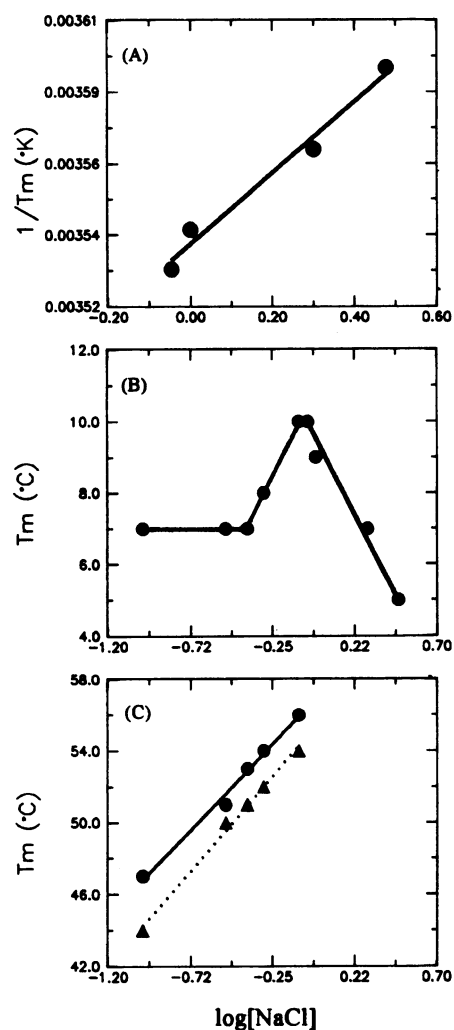


Figure 7. (A) Linear plot according to 22, $(1/T_m)$ versus $\log[\text{NaCl}]_{0.9-3 \text{ M}}$ at pH 7.0, 0.01 M cacodylate, for dissociation of third strand. (B) Plot of T_m versus $\log[\text{NaCl}]_{0.1-3 \text{ M}}$ at pH 7.0, 0.01 M cacodylate, for dissociation of third strand. (C) Plot of T_m versus $\log[\text{NaCl}]_{0.1-0.8 \text{ M}}$ at pH 7.0, 0.01 M cacodylate, for dissociation of duplex in triplex solution (●), and duplex in duplex solution (▲).

Between 0.4 and 0.9 M NaCl the dominant effect of increasing Na^+ concentration is presumably to contribute to triplex stability by shielding the negative charges of the three phosphodiester backbones; yet, over that range $\frac{\partial T_m}{\partial \log[\text{Na}^+]}$ is 10°C (Fig. 7B), relative to a value of 11°C (Fig. 7C) for the duplex, a value in good agreement for oligomers of this length. Dependence of T_m on $\log[\text{Na}^+]$ has been shown to fall off sharply with decreasing strand length, N , in the range $16 \leq N \leq 44$, e.g., for $d(\text{T-A})_9$, $\frac{\partial T_m}{\partial \log[\text{Na}^+]} = 12^\circ\text{C}$ (33). Blake *et al.* (34) showed much higher salt dependence of triplex stability, $\frac{\partial T_m}{\partial \log[\text{Na}^+]} = 31^\circ\text{C}$, for the analogous polymer triplex with uncharged homopyrimidine third strand residues [poly(U:A·U)] in comparison to 'average' duplex polymer DNA that has a value of 18°C (35,36). It must be that the salt dependence of our triplex is reduced because the net repulsive energy in the backbone is partially counterbalanced

by the positive charges on the third strand dC residues. Moreover, saturation is not observed at higher NaCl concentration, as is the case for poly(U:A·U), presumably because the ionic interaction between the Hoogsteen C⁺:G base pair is destabilized by still higher monovalent cation concentration, $\frac{\partial T_m}{\partial \log[\text{Na}^+]_{0.9 \text{ to } 3\text{M}}} = -9^\circ\text{C}$ (Fig. 7B). This inverse salt dependence has not been observed previously (37,38) as earlier work only examined salt dependence below 1 M NaCl. Plum *et al.* (37) determined $\frac{\partial T_m}{\partial \log[\text{Na}^+]_{0.2 \text{ to } 1\text{M}}} = 12^\circ\text{C}$ for melting of the third strand 5'-TTTTCTCTCTCTCT-3' from a core homopurine-homopyrimidine duplex with 21 base pairs. Our value of 10°C over an equivalent salt range is similar.

From equation 22 a plot of $\frac{1}{T_m}$ vs $\log[\text{NaCl}]_{0.9 \text{ to } 3\text{M}}$ (Fig. 7A) shows positive logarithmic dependence at pH 7.0 ($Y = 1.1 \times 10^{-4}\text{K}^{-1} X$). Substituting for $Z_1 = 33$ and $\Delta H^\circ_1 = 2.7 \text{ kcal.mol}^{-1}$ phosphate at 1 M NaCl into 22, one obtains $\Delta n_1 = -4$. Similarly at 2 M NaCl with $\Delta H^\circ_1 = 3.3 \text{ kcal.mol}^{-1}$ phosphate, $\Delta n_1 = -5$ and at 3 M NaCl with $\Delta H^\circ_1 = 5.6 \text{ kcal.mol}^{-1}$ phosphate, $\Delta n_1 = -9$.

In triplexes without protonated residues in the third strand, Δn_1 is positive as the triplex has a higher charge density than its core duplex; in that event, third strand dissociation should result in release of Na⁺. For this triplex, however, the positive charges on the dC residues of the third strand reduce the net negative charge of the triplex. Hence, on third strand dissociation above 0.9 M NaCl at pH 7.0, there is a net uptake of Na⁺ by the duplex and single strand. Confirmation that the protons on the dC residues contribute to shielding, i.e., reduce the net negative charge on the triplex, comes from the negative values for Δn_1 (uptake of Na⁺) obtained on dissociating the third strand from the core duplex at pH 7.0. Increasing NaCl concentration should favor the dissociation (Le Châteliers principle), which is what is observed in the form of decreasing triplex stability. Thus, the inverse dependence of triplex stability on NaCl concentration above 0.9 M NaCl provides additional evidence that the dC residues are protonated at pH 7.0.

Hydrogen ion dependence of third strand binding

Figure 8 shows negative dependence of T_m for third strand dissociation on pH, i.e., with $\frac{1}{T_m}$ decreasing linearly with -pH ($Y = -1.08 \times 10^{-4}\text{K}^{-1} X$). Substituting $\Delta H^\circ = 116 \text{ kcal.mol}^{-1}$ oligomer at pH 7.0 into equation 23, one obtains $\Delta n_2 = 5.5$, i.e., on dissociating the third strand at pH 7.0, 5.5 protons are released into solution. This value equals 1 H⁺ per third strand dC residue if the likelihood of bound third strands with dangling 5' dC and 3' dT residues is the same (see Fig. 11 and Discussion). It is not surprising therefore that increasing hydrogen ion concentration favors triplex stability. While this pH dependence has been widely observed, the number of protons involved in the transition has been underestimated previously (11). Quantitation in that work was based upon $\frac{dT_m}{d(\text{pH})} = \Delta H^\circ + \frac{2.3 R(T_m)^2}{\Delta H^\circ_{\text{obs}}}$ by Record *et al.* (23), which differs from our equation 23 by a factor of one half because it does not take into account the shielding contribution of protonated dC residues in the triplex. For example, the binding of d(mCTTmCmCTmC mCTmCT) (mC ≡ d 5-methylC residues) to duplex was calculated (11) to involve three protons whereas use

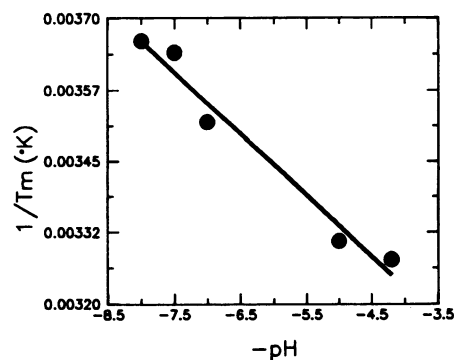


Figure 8. Linear plot according to 23, $(1/T_m)$ versus -pH in mixing buffer, for dissociation of third strand.

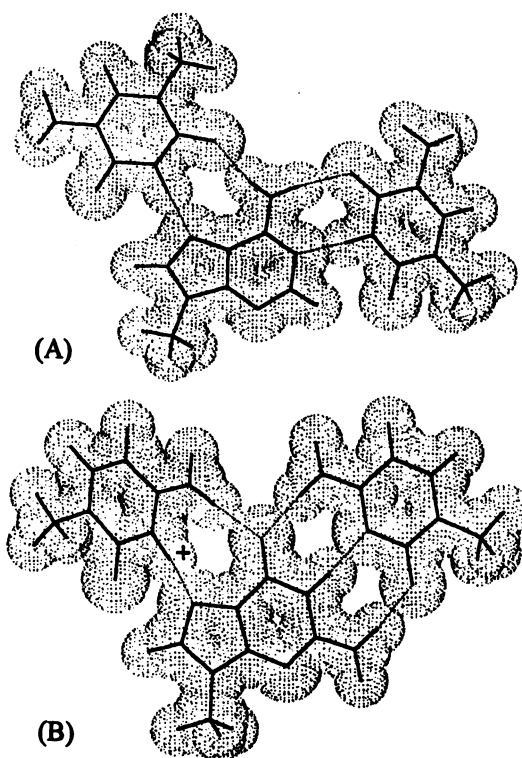


Figure 9. Energy minimized structures of isostructural base triplets between third strand pyrimidine residues and target Watson-Crick base pairs: (A) T:A:T. H-bond distances from left to right are 2.81, 2.87, 2.87 and 2.83 Å; (B) C⁺:G:C. H-bond distances from left to right are 2.66, 2.83, 2.85, 2.86 and 2.83 Å.

of equation 23 gives a value of six protons, which equals the number of third strand dC residues.

It is possible to calculate the free energy associated with transfer of H⁺ from aqueous solution to the third strand dC residues at various pH values using $\Delta G_{\text{pK}_a} = 2.303 RT\Delta\text{pK}_a$, where ΔpK_a is essentially the difference between 4.6 (pK_a of dCMP) and the pH of the bulk solution. This will be favorable if the pH of the solution is below 4.6 or unfavorable if above. At 25°C, $\Delta G_{\text{pK}_a} = -0.6 \text{ kcal.mol}^{-1} \text{ H}^+$ at pH 4.2, 0.6 at pH 5.0, 3.3 at pH 7.0 and 4.0 at pH 7.5. The increasingly large positive values as pH rises above 5.0 indicate that third strand association with

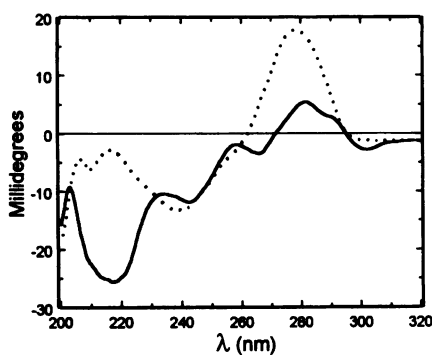


Figure 10. Comparison of CD spectra of the duplexes $d(A-G)_6 \cdot d(C^+ \cdot T)_6$ at pH 4.2 (—) and $d(A-G)_6 \cdot d(C \cdot T)_6$ at pH 7.0 (···) in mixing buffer titrated to the indicated pH.

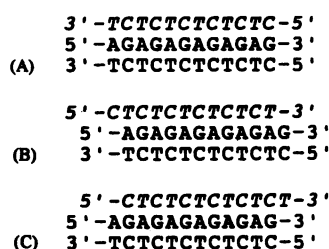


Figure 11. Conceivable binding motifs of the third strand, shown as the top strand in italics. (A) Third strand binding antiparallel requires reverse Hoogsteen base pairing. (B) Third strand binding parallel with Hoogsteen base pairing and a 5' overhang. (C) Third strand binding parallel with Hoogsteen base pairing and a 3' overhang. Strand orientation is expressed with reference to that of the homopurine strand (middle strand) of the target duplex.

duplex requires significant favorable interactions for triplex to form. For the triplex at pH 7.0, at T_m (11°C), $\Delta G_{total} = 0 = \Delta G_{pKa} + \Delta G_{structural}$, where $\Delta G_{structural}$ is the favorable free energy contribution resulting from the third strand-duplex interactions. With $\Delta G_{pKa} = 3.1 \text{ kcal.mol}^{-1} \text{ H}^+$ at 11°C, $\Delta G_{structural} = -18.6 \text{ kcal.mol}^{-1}$ oligomer. Since we have shown that triplex formation requires protonation of the third strand dC residues, a significant contribution to $\Delta G_{structural}$ must come from elimination of the lone pair repulsion between N3 of dC and N7 of dG by formation of an ionic H-bond (Fig. 10), and the favorable Coulombic attraction between the protonated dC residues and the surrounding negatively charged phosphodiester backbones of the three strands. These observations provide further evidence for the protonated state of third strand dC residues in C:G·C triplets at neutrality, i.e., $C^+ : G \cdot C$.

Energy minimized structures of T:A·T and $C^+ : G \cdot C$ versus C:G·C

The energy minimized structure for the isolated base triplet T:A·T, shown in Figure 9A, was obtained after 309 search directions and 686 single point calculations, resulting in an energy minimum of $-90.5 \text{ kcal.mol}^{-1}$. The space filling model shows four H-bond 'contacts', all within standard H-bond distances.

The comparable energy minimized structure for $C^+ : G \cdot C$ (Fig. 9B) was obtained after 265 search directions and 561 single point

calculations, resulting in an energy minimum of $-169.0 \text{ kcal.mol}^{-1}$. The space filling model shows five H-bond 'contacts', all within standard H-bond distances. Noteworthy is the significantly shorter ionic H-bond of 2.66 \AA versus 2.84 ± 0.02 for the others, showing the additional stability arising from the significantly larger electrostatic contribution to this H-bond.

In contrast, no reasonable structure could be obtained for the isolated base triplet C:G·C. Since all the energy minimizations were done with no constraints, the neutral Hoogsteen N1-methylcytosine was apparently forced away from the N9-methylguanine, resulting in no realistic structure. The repulsion between the lone pair electrons on N3 of the Hoogsteen cytosine and on N7 of guanine results in an energetically very unstable Hoogsteen C:G interaction that would require large amounts of compensatory stacking energy not likely to result from the overlap of dT and dC residues in the third strand. As expected, the Watson-Crick G·C base pair in these base triplets remained normal after these minimizations. Thus, there is a clear electrostatic basis for the requirement for protonation of dC in order to form a $C^+ : G \cdot C$ base triplet at any pH value.

DISCUSSION

Condensation-screening theory

Our derivation for the salt dependence of T_m without taking protonated residues into account, **20**, is the same as that obtained by Manning (22). [See (54,55) for comparison of the Poisson-Boltzmann equation and the Debye-Hückel approximation as applied to polyelectrolytes of the DNA type. The work of Bleam *et al.* (56) has shown that for DNA the fractional extent of neutralization ($\theta_{Na^+} = 0.75 \pm 0.1$) is in very good agreement with that predicted by counterion condensation theory ($\theta_{Na^+} = 0.76$). Thus, in spite of the simple model used in counterion condensation theory, it gives accurate calculation of many polyelectrolyte phenomena for a variety of systems (56-59).] When Record *et al.* (23) analyzed the dependence of T_m on salt concentration for protonated helices, they obtained for the dependence of T_m on pH (their equation 22)

$$\frac{dT_m}{d(\text{pH})} = (\Delta H^+) \frac{2.3 R(T_m)^2}{\Delta H^{\circ}_{obs}} \quad \text{A}$$

where ΔH^+ is the number of H^+ involved in the helix-coil transition.

In contrast, we obtain

$$\frac{dT_m}{d(\text{pH})} = \frac{(\Delta H^+) 2.3 R(T_m)^2}{2 \Delta H^{\circ}_{obs}} \quad \text{B}$$

where the factor of one half results from explicit inclusion of electrostatic shielding by H^+ (i.e. $\Delta G_{el \text{ H}^+}$ of our **15**). Although we have developed our analysis for the triplex at pH 7, it is easily generalized to any coil to helix transition involving proton uptake. For such cases **B** is the same, but the expression for ΔH^+ , **13**, would be different e.g.,

$$2 \text{ poly(A)} + 2 \text{ H}^+ \rightarrow \text{poly(A}^+ \cdot \text{A}^+) \text{ and } \Delta H^+ = Z_2 \left(\frac{1}{2\epsilon_{(S_1)}} + \frac{1}{2\epsilon_{(S_2)}} - \frac{1}{\epsilon_{(D)}} \right).$$

As is the case for the triplex we have studied and the similar one studied by Xodo *et al.* (11), use of **B** results in exact agreement with the number of H^+ involved in third strand binding. These results show that all the third strand dC residues must be

protonated, even at pH 7. The importance of all the third strand dC residues requiring H⁺ upon binding has also been shown for dC residues that are adjacent d(TTC⁺C⁺C⁺TC⁺TTC⁺C⁺C⁺C⁺) (39).

The difference in the number of H⁺ released when poly(A⁺·A⁺) is melted at pH 4.2 and 5.3 is 0.55 (40). Using the data and A from (23), ΔH^+ was calculated to be 0.2 (23); however, using our equation B, we obtain $\Delta H^+ = 0.4$, much closer to the value observed experimentally.

UV-spectroscopy

The spectral components contributing to the UV-absorbance difference on third strand dissociation have been identified, and it has been explicitly shown that deprotonation of dC residues is the major spectral component at pH 7.0. This method of spectral analysis should prove useful for current work on the acid induced structures of poly[d(C)] and poly[r(C)] (41) and of d(C-T)_n and d(C_nT_n) (42–44) in which dC residues are required in the base pairing schemes, C⁺·C, C⁺·T, and C·T for a number of proposed novel structures (parallel and antiparallel duplexes, tetraplexes).

Enthalpy values for dissociation of third strand and duplex

For the duplex, d(A-G)₆·d(C-T)₆, in a duplex mixture over a variety of conditions, 0.15 M NaCl/0.005 M MgCl₂/pH 5.0–8.5, and 0.1–3.0 M NaCl/pH 7.0, our mean ΔH°_{obs} value of about –6 kcal.mol^{–1} base pair is in very good agreement with other reported mean ΔH° values, e.g., for a similar homopurine–homopyrimidine 21 base pair duplex, $\Delta H^{\circ} = -6$ kcal.mol^{–1} base pair obtained by DSC (37). Unlike the sensitivity to pH and ionic conditions indicated by the ΔH° values for the triplex, the ΔH° values show that the interactions that stabilize the Watson–Crick duplex are not similarly sensitive.

However, our ΔH°_{obs} values for dissociation of third strand do vary with solution conditions, showing that the interactions of these Hoogsteen base pairs are quite sensitive to ionic strength and pH and that this third strand binding interaction is stronger than that between the strands of a Watson–Crick duplex. Our ΔH°_{obs} values for the dissociation of the third strand include all the enthalpic components that contribute to the transition: dissociation of the Hoogsteen base pairs, T:A and C⁺:G; deprotonation of the dC⁺ residues (when the solution pH > 4.6) and any additional enthalpy changes occurring in the core Watson–Crick duplex, i.e., A → B transition. The literature contains a variety of ΔH° values for the Hoogsteen base pairs of similar deoxytriplexes: –6.6 by UV and after subtracting the estimated enthalpy contribution from protonation of the dC⁺ residues (45), –5.8 by DSC and UV and after subtracting the estimated enthalpy contribution from protonation of the dC⁺ residues (46), –5 by UV (47), –4.2 by UV (48), –2.0 by calorimetry and –6 kcal.mol^{–1} Hoogsteen base pair by UV (37). This spread of values may result from differences in oligomer sequence (stacking interactions); end effects due to variation in length of strands, including in some cases differences in the third strand and core duplex length; various solution conditions (pH, ionic strength, different cations); and variations in the methods and models used to obtain the enthalpy values. [In this connection, we take issue with the notion that spectroscopically obtained enthalpy values must be incorrect when they are not

similar to calorimetrically obtained values. It is the prevailing view that calorimetrically obtained values are correct because they are obtained from a direct enthalpic measurement, whereas spectroscopically derived values require assumption of a model (37,60). However, these differences in mode of enthalpic estimation could mean that they measure different enthalpic events. The calorimetric measurement subtracts the enthalpic changes occurring in the reference solution (equivalent solution with no oligonucleotide) from those occurring in the sample. In the spectroscopic method the reference solution does not contribute to the absorbance difference at the wavelength of observation, in this case 255 nm, and therefore does not affect the transition curve. Different results from the two methods may also be due to the different oligomer concentrations used, calorimetry generally requiring 20 times more concentrated solutions. Equivalent ΔH° values for third strand dissociation in solutions of very different oligomer concentration can only be expected if their water activity is the same and if water does not contribute to the enthalpy change on third strand dissociation; neither of these assumptions is correct. This has been confirmed by calorimetric studies showing a significant enthalpic contribution from reorganization of water during complexation in aqueous solution between protein–nucleotide, protein–peptide, protein–carbohydrate, and small molecule–small molecule systems (61). Also, we have shown that water plays an important role in triplex formation (Lavelle, L. and Fresco, J.R., in preparation.) A recent paper by Wilson *et al.* (49) has shown that calorimetrically-obtained enthalpy values, only for third strands with C residues, vary significantly with the type of buffer used and the pH [for a third strand (19 mer) containing only three dC residues the enthalpy values vary from –2.9 to –5 kcal.mol^{–1} base triplet].

Ionic strength dependence

If the third strand dC residues in the triplex were uncharged at pH 7.0, then one would expect a positive ionic strength dependence of triplex stability over a broad range of ionic strength, due to the high negative charge density arising from the negatively charged phosphates on the three strands. Such ionic strength dependence of stability is the norm for duplexes and triplexes with uncharged bases, e.g., poly(U:A·U) (34). In contrast, inverse salt dependence of T_m at moderate ionic strengths is observed with duplexes stabilized by ionic interactions, as in the case of poly(C⁺·C) (25,50) and poly(A⁺·A⁺) (51). Similarly, we observe that increasing NaCl concentration above 0.9 M destabilizes third strand binding, and we attribute this reversal of salt dependence to increased shielding by the Na⁺, resulting in a reduced affinity of the dC residues for H⁺ and a decrease in the electrostatic attraction between the C⁺:G Hoogsteen base pair and also the dC⁺ residues and the phosphodiester backbone of the duplex. We do not attribute this reduction in T_m to the higher concentrations of Cl[–], as the duplex at these high concentrations (1 to 3 M NaCl) shows no reduction in stability (Table 1). In this regard, there is some confusion in the literature as to the effect that high concentrations of anions have on duplex stability. Our results confirm those of Hamaguchi and Geiduschek (52), who showed that DNA has a constant T_m of 90°C at high ionic strengths of up to 4 M NaCl; i.e., there is no T_m dependence on Cl[–] concentration, unlike other anions that were shown to decrease duplex stability and were classed as hydrophobic bond breaking agents and arranged in a chaotropic series by those authors.

Table 1. Thermodynamic parameters for dissociation* of the third strand from the target duplex and for dissociation* of the duplex

Sample	Conditions	$\Delta H^{\circ}_{\text{obs}}$ kcal.mol ⁻¹ of base pair	$\Delta H^{\circ}_{\text{obs}}$ kcal.mol ⁻¹ of oligomer	$\Delta S^{\circ}_{\text{obs}}$ kcal.mol ⁻¹ .K ⁻¹ of oligomer	$\Delta G^{\circ}_{\text{obs,298}}$ kcal.mol ⁻¹ of oligomer	T _m °C
Triplex Mixture ^a 1st Transition	pH 4.2	8.9	107	0.35	2.5	32
	5.0	7.3	88.1	0.29	1.2	29
	7.0	9.7	116	0.41	-5.7	11
	7.5	8.1	97.5	0.36	-8.5	1
	8.0	-	-	-	-	0
Triplex Mixture ^b 1st Transition	M NaCl 0.1	7.2	86.0	0.31	-5.5	7
	0.3	6.6	79.1	0.28	-5.1	7
	0.4	7.1	85.4	0.31	-5.5	7
	0.5	7.3	88.1	0.31	-5.3	8
	0.8	6.4	76.5	0.27	-4.1	10
	0.9	5.9	70.9	0.25	-3.8	10
	1.0	7.3	87.6	0.31	-5.0	9
	2.0	9.2	110	0.39	-7.1	7
3.0	15.4 [†]	185	0.67	-13.3	5	
Triplex Mixture ^a 2nd Transition	pH 4.2	13.6 [†]	163	0.49	18.0	62 [†]
	5.0	9.3	112	0.35	8.7	50
	7.0	8.2	98.7	0.31	7.6	50
	7.5	7.6	91.4	0.28	7.1	50
	8.0	8.2	98.4	0.31	7.6	50
	8.5	8.8	106	0.33	7.9	49
Triplex Mixture ^b 2nd Transition	M NaCl 0.1	6.8	82.0	0.26	5.6	47
	0.3	7.6	91.3	0.28	7.3	51
	0.4	7.8	93.3	0.29	8.0	53
	0.5	6.6	78.9	0.24	7.0	54
	0.8	7.4	88.8	0.27	8.4	56
	0.9	7.8	93.1	0.28	8.8	56
	1.0	6.8	82.0	0.25	7.3	54
	2.0	7.8	93.7	0.29	8.3	54
	3.0	8.7	104	0.32	10.1	57
Duplex Mixture ^a	pH 4.2	8.4 [†]	101	0.31	9.8	57 [†]
	5.0	5.7	67.9	0.21	4.9	48
	7.0	6.4	76.9	0.24	5.5	48
	7.5	6.2	74.8	0.23	5.4	48
	8.0	6.6	79.1	0.25	5.7	48
	8.5	6.3	75.6	0.24	5.4	48
Duplex Mixture ^b	M NaCl 0.1	5.6	67.3	0.21	4.0	44
	0.3	5.8	69.0	0.21	5.3	50
	0.4	6.1	72.9	0.22	5.9	51
	0.5	5.7	68.3	0.21	5.7	52
	0.8	5.8	69.4	0.21	6.1	54
	0.9	5.8	69.6	0.21	6.2	54
	1.0	6.0	72.0	0.22	6.2	53
	2.0	5.7	68.7	0.21	5.7	52
	3.0	5.7	68.8	0.21	5.7	52

*The more positive the $\Delta G^{\circ}_{\text{obs}}$ the more stable the triplex or duplex.

^a0.01 M cacodylate/0.15 M NaCl/0.005 M MgCl₂.

^bpH 7.0/0.01 M cacodylate.

[†]For discussion of these values see Results section, Thermodynamic parameters for the triplex and duplex transitions.

Third strand orientation and register

Binding of the homopyrimidine third strand via reverse Hoogsteen base pairing is not known to occur, i.e., with the third strand antiparallel to the Watson–Crick homopurine strand (Fig. 11A). Binding of the third strand parallel to the homopurine strand has been proposed from fiber diffraction data and modeling (8,53) and confirmed by NMR for the triplex d(T-C)₄:d(G-A)₄·d(T-C)₄ (15). But even with parallel third strand orientation via Hoogsteen base pairing, two alternative registers are possible. The third strand must be displaced, with either a dangling dC residue at the 5' end (Fig. 11B) or a dangling dT residue at the 3' end (Fig. 11C). While both of these binding arrangements have 11 base pair interactions, the structure with the 3' overhang is more likely

under acidic conditions (Fig. 11C), whereas the 5' overhang is more likely at neutrality, since the 5' third strand dC residue need not then be protonated (Fig. 11B). As noted above, an equilibrium between these alternatives is consistent with the value of 5.5 calculated for Δn_2 .

CONCLUSION

We have shown that protonation of third strand dC residues is required for d(C-T)₆ to interact with [d(A-G)₆·d(C-T)₆] to form a triplex at neutrality or above. In this respect, formation of this triplex is mediated by a 'proton switch'. Not surprisingly, under such conditions third strand dissociation is cooperative, occurring with release of H⁺ ions. An electrostatic rationale is provided for

the essentiality of dC residue protonation. The reason is not so much the formation of the second H-bond *per se*, as it is to prevent the repulsion between the lone pair electrons on N3 of the third strand dC residues and on N7 of the dG residues of the target Watson-Crick base pairs. The understanding developed here for the C⁺:G·C base triplet should provide insights regarding the properties of other base triplets with analogous potential for ionizable third strand residues, as well as of other structures with base-base interactions involving ionized residues.

ACKNOWLEDGEMENTS

This work was supported by NIH grant (GM 42936) to J.R.F., and a Berlex Pre-Doctoral Fellowship from Berlex Corp., a Pre-Doctoral Traineeship from NIH grant (GM 08309), an Autodesk educational software grant from Autodesk Corp. and a gift of AXUM 3.0 from TriMetrix Corporation to L.L.

REFERENCES

- Wells, R. D., Collier, D. A., Hanvey, J. C., Shimizu, M. and Wohlrab, F. (1988) *FASEB J.* **2**, 2939–2949.
- Htun, H. and Dahlberg, J. E. (1989) *Science* **243**, 1571–1576.
- Moser, H. E. and Dervan, P. B. (1987) *Science* **238**, 645–650.
- Fresco, J. R. (1963) in Vogel, H. J., Bryson, V. and Lampen, J. O. (Eds), *Informational Macromolecules*. pp. 121–142, Academic Press, New York.
- Lipsett, M. N. (1964) *J. Biol. Chem.* **239**, 1256–1260.
- Morgan, A. R. and Wells, R. D. (1968) *J. Mol. Biol.* **37**, 63–80.
- Thiele, D. and Guschlbauer, W. (1971) *Biopolymers*. **10**, 143–157.
- Arnott, S., Bond, P. J., Selsing, E. and Smith, P. J. C. (1976) *Nucleic Acids Res.* **3**, 2459–2470.
- Mirkin, S. M., Lyamichev, V. I., Drushlyak, K. N., Dobrynin, V. N., Filippov, S. A. and Frank-Kamenetskii, M. D. (1987) *Nature* **330**, 495–497.
- Letai, A. G., Palladino, M. A., Fromm, E., Rizzo, V. and Fresco, J. R. (1988) *Biochemistry* **27**, 9108–9112.
- Xodo, L. E., Manzini, G., Quadrifoglio, F., van der Marel, G. A. and van Boom, J.H. (1991) *Nucleic Acids Res.* **19**, 5625–5631.
- Hanvey, J. C., Williams, E. M. and Besterman, J. M. (1991) *Antisense Res. Dev.* **1**, 307–317.
- Singleton, S. F. and Dervan, P. B. (1992) *Biochemistry* **31**, 10995–1003.
- Rajagopal, P. and Feigon, J. (1989) *Nature* **339**, 637–640.
- Rajagopal, P. and Feigon, J. (1989) *Biochemistry* **28**, 7859–7870.
- Cheng, Y. K. and Pettitt, B. M. (1992) *Prog. Biophys. Mol. Biol.* **58**, 225–257.
- Sklenár, V. and Feigon, J. (1990) *Nature* **345**, 836–838.
- AXUM 3.0, (1993) TriMetrix Corporation, 444 NE Ravenna Blvd., Suite 210, Seattle, WA 98115.
- HyperChem 2.0 (1992) Autodesk Corporation, Scientific Modeling Division, 2320 Marinship Way, Sausalito, CA 94965.
- Singh, U. C., Weiner, P. K., Caldwell, J. and Kollman, P. A. (1989) University of California, San Francisco, CA.
- Manning, G. S. (1969) *J. Chem. Phys.* **51**, 924–933.
- Manning, G. S. (1972) *Biopolymers* **11**, 937–949.
- Record, M. T. Jr., Woodbury, C. P. and Lohman, T. M., (1976) *Biopolymers* **15**, 893–915.
- Adams, A., Lindahl, T. and Fresco, J. R. (1967) *Proc. Natl. Acad. Sci. USA* **57**, 1684–1691.
- Akinrimisi, E. O., Sander, C. and Ts'o, P. O. P. (1963) *Biochemistry* **2**, 340–344.
- Inman, R. B. (1964) *J. Mol. Biol.* **9**, 624–637.
- Liu, K., Miles, H. T., Frazier, J. and Sasisekharan, V. (1993) *Biochemistry* **32**, 11802–11809.
- Hoogsteen, K. (1963) *Acta Crystallogr.* **16**, 907–916.
- Ornstein, R. L. and Fresco, J. R. (1983) *Proc. Natl. Acad. Sci. USA* **80**, 5171–5175.
- Allen, L. C. (1975) *J. Am. Chem. Soc.* **97**, 6921–6940.
- Burstein, K. Y. and Isaev, A. N. (1984) *Theoret. Chim. Acta (Berl.)* **64**, 397–401.
- Pullman, B., Claverie, P. and Caillet, J. (1967) *Proc. Natl. Acad. Sci. USA* **57**, 1663–1669.
- Elson, E. L., Scheffler, I. E. and Baldwin, R. L. (1970) *J. Mol. Biol.* **54**, 401–415.
- Blake, R. D., Massoulié, J. and Fresco, J. R. (1967) *J. Mol. Biol.* **30**, 291–308.
- Dove, W. F. and Davidson, N. (1962) *J. Mol. Biol.* **5**, 467–478.
- Record, M. T., Jr. (1967) *Biopolymers*. **5**, 975–992.
- Plum, G. E., Park, Y. W., Singleton, S. F., Dervan, P. B. and Breslauer, K. J. (1990) *Proc. Natl. Acad. Sci. USA* **87**, 9436–9440.
- Völker, J. and Klump, H. H. (1994) *Biochemistry* **33**, 13502–13508.
- Mirkin, S. M. and Frank-Kamenetskii, M. D. (1994) *Annu. Rev. Biophys. Biomol. Struct.* **23**, 541–576.
- Holcomb, D. N. and Timasheff, S. N. (1968) *Biopolymers* **6**, 513–529.
- Antao, V. P. and Gray, D. M. (1993) *J. Biomol. Struct. Dyn.* **10**, 819–839.
- Gehring, K., Leroy, J. L. and Gueron, M. (1993) *Nature* **363**, 561–565.
- Jaishree, T. N. and Wang, A. H. J. (1993) *Nucleic Acids Res.* **21**, 3839–3844.
- Leroy, J. L., Gehring, K., Kettani, A. and Gueron, M. (1993) *Biochemistry* **32**, 6019–6031.
- Manzini, G., Xodo, L. E., Gasparotto, D., Quadrifoglio, F., van der Marel, G. A. and van Boom, J. H. (1990) *J. Mol. Biol.* **213**, 833–843.
- Xodo, L. E., Manzini, G. and Quadrifoglio, F. (1990) *Nucleic Acids Res.* **18**, 3557–3564.
- Rougée, M., Faucon, B., Mergny, J. L., Barcelo, F., Giovannangeli, C., Garestier, T. and Helene, C. (1992) *Biochemistry* **31**, 9269–9278.
- Pilch, D. S., Brousseau, R. and Shafer, R. H. (1990) *Nucleic Acids Res.* **18**, 5743–5750.
- Wilson, W. D., Hopkins, H. P., Mizan, S., Hamilton, D. D. and Zon, G. (1994) *J. Am. Chem. Soc.* **116**, 3607–3608.
- Guschlbauer, W. (1967) *Proc. Natl. Acad. Sci. USA* **57**, 1441–1448.
- Michelson, A. M., Massoulié, J. and Guschlbauer, W. (1967) *Progr. Nucleic Acid Res.* **6**, 83–141.
- Hamaguchi, K. and Geiduschek, E. P. (1962) *J. Am. Chem. Soc.* **84**, 1329–1338.
- Arnott, S. and Selsing, E., (1974) *J. Mol. Biol.* **88**, 509–521.
- Frank-Kamenetskii, M. D., Anshelevich, V. V. and Lukashin, A. V. (1987) *Sov. Phys. Usp.* **30**, 317–330.
- Anderson, C. F. and Record, M. T. Jr. (1990) *Annu. Rev. Biophys. Biomol. Struct.* **19**, 423–465.
- Bleam, M. L., Anderson, C. F. and Record, M. T. Jr. (1980) *Proc. Natl. Acad. Sci. USA* **77**, 3085–3089.
- Granot, J. and Kearns, D. R. (1982) *Biopolymers* **21**, 203–218.
- Braunlin, W. H., Anderson, C. F. and Record, M. T. Jr. (1987) *Biochemistry* **26**, 7724–7731.
- Padmanabhan, S., Richey, B., Anderson, C. F. and Record, M. T. Jr. (1987) *Biochemistry* **27**, 4367–4376.
- Marky, L. A. and Breslauer, K. J. (1987) *Biopolymers* **26**, 1601–1620.
- Chervenak, M. C. and Toone, E. J. (1994) *J. Am. Chem. Soc.* **116**, 10533–10539.

This is paper no. 21 in the series entitled Polynucleotides, of which the last is Dolinnaya, N.G, Braswell, E.H., Fossella, J.A., Klump, H. and Fresco, J.R. (1993) *Biochemistry*, **32** 10263–10270.